

Cover Page



Universiteit Leiden



The handle <http://hdl.handle.net/1887/28971> holds various files of this Leiden University dissertation

Author: Rosalia, Rodney Alexander

Title: Particulate based vaccines for cancer immunotherapy

Issue Date: 2014-10-02

Chapter 2

Dendritic cells process synthetic long peptides better than whole protein, improving antigen presentation and T-cell activation

Rodney A. Rosalia, Esther D. Quakkelaar, Anke Redeker, Selina Khan, Marcel Camps, Jan W. Drijfhout, Ana Luisa Silva, Wim Jiskoot, Thorbald van Hall, Peter A. van Veelen, George Janssen, Kees Franken, Luis J. Cruz, Angelino Tromp, Jaap Oostendorp, Sjoerd H. van der Burg, Ferry Ossendorp & Cornelis J.M. Melief

Abstract

The efficiency of antigen (Ag) processing by dendritic cells (DCs) is vital for the strength of the ensuing T-cell responses. Previously we and others have shown that in comparison to protein vaccines, vaccination with synthetic long peptides (SLPs) has shown more promising (pre-)clinical results. Here we studied the unknown mechanisms underlying the observed vaccine efficacy of SLPs. We report an in vitro processing analysis of SLPs for MHC class I and class II presentation by murine DCs and human monocyte-derived DC (MoDCs). Compared to protein, SLPs were rapidly and much more efficiently processed by DCs, resulting in an increased presentation to CD4⁺ and CD8⁺ T cells. The mechanism of access to MHC class I loading appeared to differ between the two forms of Ag. Whereas whole soluble protein Ag ended up largely in endo-lysosomes, SLPs were detected very rapidly outside the endo-lysosomes after internalization by DCs, followed by proteasome- and TAP-dependent MHC class I presentation. Compared to the slower processing route taken by whole protein Ags, our results indicate that the efficient internalization of SLPs, accomplished by DCs but not by B or T cells and characterized by a different and faster intracellular routing, leads to enhanced CD8⁺ T-cell activation.

Introduction

DCs are the major antigen (Ag) presenting cells (APCs) of the immune system and initiate adaptive T-cell responses¹. Therapeutic vaccination in cancer immunotherapy aims at the induction of potent effector CD4⁺ and CD8⁺ T-cell responses able to target and eradicate malignant cells. Vaccination with properly folded protein Ag efficiently induces CD4⁺ T helper cell responses that can exert effector function by themselves, and strongly promotes (neutralizing) antibody formation and has therefore successfully been applied for prophylactic vaccination against viral infections²⁻⁴. Although protein vaccines can induce CD8⁺ T-cell responses⁵, efficient anti-tumor immune responses require a more robust and efficient induction of potent cytotoxic CD8⁺ T cells. However, improvement of the quality and quantity of CD8⁺ T-cell responses by vaccination remains a major challenge^{6,7}. Our group has previously reported successful induction of potent CD4⁺ and CD8⁺ T-cell responses in preclinical models and patients with (pre-)malignant disease of the cervix via therapeutic vaccination with synthetic long peptides (SLPs) of the E6 and E7 oncoproteins of high risk HPV16⁸⁻¹⁰. The SLPs used as vaccines in these studies are overlapping synthetic peptides of 15–35 amino acids that i) Cover the entire sequence of the native protein Ag to which an immune response is targeted and ii) Require internalization and processing by DCs for optimal presentation in MHC class I and class II molecules¹¹ iii) Do not require HLA-typing as ingestion by antigen-presenting cells of overlapping strands of peptides allows epitope selection *in vivo* based on the patient's own HLA-profile iv) Facilitates simultaneous priming of T cells against multiple dominant and subdominant epitopes stimulating a broad T-cell response¹². SLP vaccines have also been used against other types of cancers. T-cell immunity was induced against p53 in patients with metastatic colorectal cancer using SLP vaccines¹³ and robust immune responses were similarly induced against NY-ESO-1 in patients with ovarian cancer¹⁴. In addition, SLP vaccines have shown promising results against other immunological diseases¹⁵⁻¹⁸. In a direct comparison, SLP vaccines were more efficient in inducing CD8⁺ T-cell responses than protein vaccines^{6,17} and lead to stronger and more effective Ag-specific immune responses¹⁹⁻²¹. The positive effects of SLP vaccines in pre-clinical models and in patients are well described, but little is known concerning the mechanisms underlying the vaccine efficacy and the intracellular processing and efficiency of MHC class I and class II presentation of SLPs. It is believed that substitution of whole protein Ag by overlapping long peptide Ag facilitates the internalization, processing and presentation of the relevant epitopes by DC¹¹. We now report studies on the uptake, intracellular localization, and efficiency of processing and MHC presentation of SLPs by

murine and human DCs, including scrutiny of the role of the proteasome, TAP and endo-lysosomal processing in MHC class I cross-presentation of SLPs. To our knowledge this is the first report presenting how DC efficiently process SLPs, for presentation to CD8⁺ T cells. We observed a distinct cellular localization of SLPs compared to protein in DC following exposure to Ag, compatible with the different kinetics and efficiency of cross-presentation and subsequent CD8⁺ T-cell activation. These results highlight the fact that SLPs behave fundamentally different from proteins as an Ag for T-cell response induction. This insight can serve as a starting point for further optimization of SLP-based vaccines.

RESULTS

Superior Ag presentation of SLPs by DCs compared with that of protein

The capacity of DCs to process and present different forms of exogenous Ag in MHC class I and II was studied by loading BMDCs with SLP-OVA_{24aa} or soluble OVA protein (OVA-protein) for 24 h and measuring B3Z CD8⁺ T-cell and KZO CD4⁺ T-cell activation. DCs loaded with SLPs potently activate B3Z and KZO T cells suggesting that SLPs is internalized and efficiently routed into the MHC class I and II Ag presentation pathways (Figure 2.1A and B). In contrast, DCs loaded with protein completely failed to activate CD8⁺ T cells but did successfully activate KZO CD4⁺ T cells, albeit with at least 64-fold lower efficiency compared to SLP-loaded DCs (Figure 2.1B). Pre-stimulation of DCs with the TLR4 ligand LPS had no effect on the MHC class I presentation of OVA-protein but improved Ag presentation of SSP-OVA_{8aa} (data not shown) and long peptide Ag (Figure 2.1C). HLA-B7-restricted presentation by human MoDCs of HIV-derived protein and SLPs was also studied. We were unable to detect cytokine production by CD8⁺ T cells co-cultured with GAG-protein-loaded DCs. In contrast, SLP-GAG_{22aa} induced significant CD8⁺ T-cell activation (see Figure 2.2 and below). Together, these data show that cross-presentation of SLPs is superior to that of proteins as examined with both mouse and human DCs.

Rapid Ag presentation of SLPs by murine and human DCs

The efficiency of SLP-processing was assessed by studying the time required for DCs to present Ag on MHC class I (H2-K^b) molecules. Murine DCs were incubated with a single concentration of SLPs, SSPs or protein for the indicated time-periods. The minimal peptide, SSPs, was rapidly presented to CD8⁺ T cells resulting in strong activation already after 1

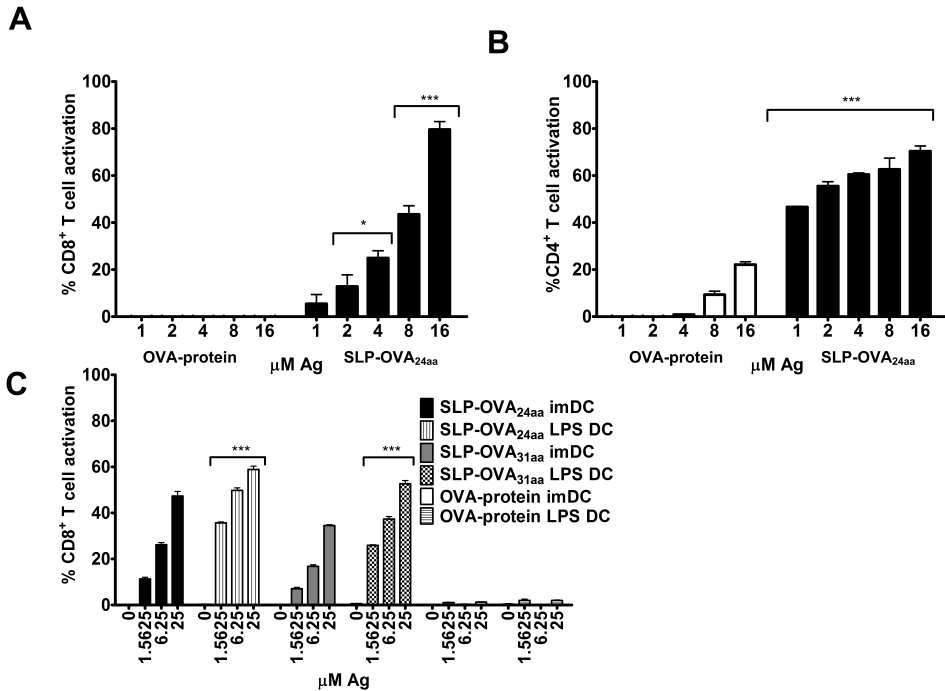


Figure 2.1 Efficient MHC class I and class II presentation by mouse DCs incubated with SLPs.

C57BL/6 x C3H F₁ BMDCs were incubated for 24 h with titrated amounts of SLP-OVA_{24aa} or OVA-protein and co-cultured overnight in the presence of (A) B3Z CD8⁺ T cells or (B) KZO CD4⁺ T cells. T-cell activation was determined as described in Materials and Methods. (C) D1 cells were pre-cultured with 10 μ g/ml LPS (LPS DC) and compared with immature DCs (imDC) in their capacity to activate B3Z T cells after 24 h incubation with Ag. Data are shown as mean + SD of 3 samples from one representative experiment representative of four (A), two (B) and three (C) experiments performed. ***P < 0.001, *P < 0.05, two-way ANOVA and Bonferroni posttests.

h. DCs loaded with SLP- also activated CD8⁺ T cells 1 h after Ag loading but with lower potency. We excluded that SLPS- were cleaved extra-cellularly, processed and loaded on MHC class I and II molecules by incubating PFA-fixed cells for with the peptide Ag and observed no cross-presentation (data not shown). DCs loaded with 10 μ M OVA-protein failed to induce significant CD8⁺ T-cell activation (Figure 2.2A). I-A^b-restricted MHC class II presentation was next studied and we observed that within 1 h of Ag incubation DC loaded with SLP-OVA_{17aa} and SLP-OVA_{31aa} activated CD4⁺ T cells with similar efficiency even though the peptides varied in length. In contrast, DC loaded with OVA-protein stimulated OT-II/CD4⁺ T cells with lower potency and it took at least 3 h of Ag loading, suggesting

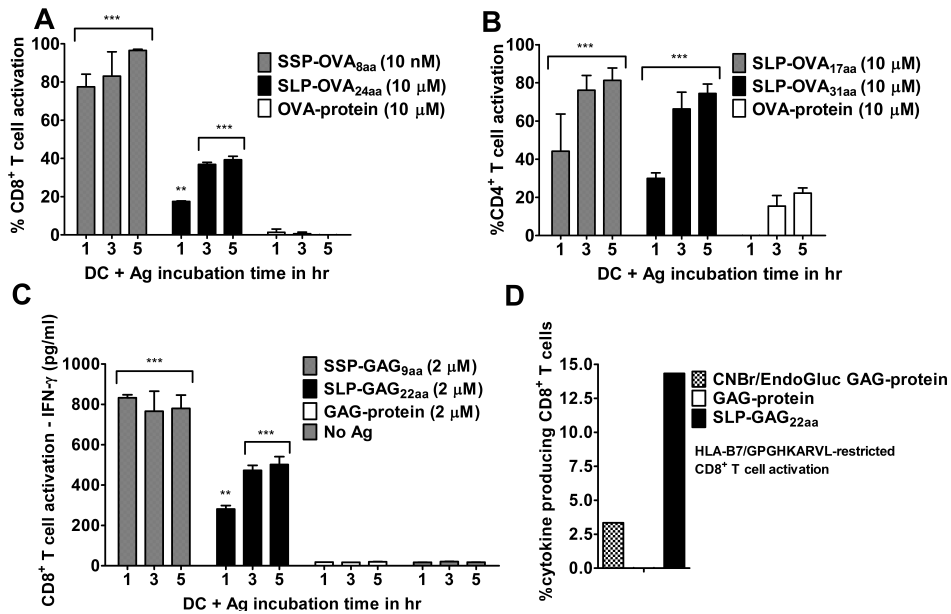


Figure 2.2 Rapid cross-presentation by mouse and human DCs loaded with SLPs compared with soluble protein.

Murine DCs were pulsed for 1, 3 or 5 h with 10 nM SSP-OVA_{8aa}, 10 μM SLP-OVA_{17aa}, SLP-OVA_{24aa}, SLP-OVA_{31aa} or OVA-protein, washed 3x times with PBS/0.2% FCS and fixed with 0.4% paraformaldehyde. Ag-loaded DCs were cultured overnight with (A) B3Z CD8⁺ T cells or (B) OT-I/II CD4⁺ T cells. (C) Human MoDCs were incubated for 1, 3 or 5 h with GAG protein, SLP-GAG_{22aa} or SLP-GAG_{9aa} (2 μM), cells fixed, and HIV-specific CD8⁺ T cells added overnight. IFN-γ production measured by ELISA was used to determine CD8⁺ T-cell activation. MoDCs were incubated for 24 h with SLP-GAG_{22aa}, soluble GAG-protein and a CNBr/EndoGluc-treated GAG-protein digest. (D) HIV-specific T cells were added and total IFN-γ- or TNF-α-producing cells were determined by flow cytometry. Data are shown as mean + SD of 3 samples from one experiment representative of three (A) or two (B, C) or from one single experiment (D). (A-C) Data were analyzed with two-way ANOVA and Bonferroni posttests, ***P < 0.001, **P < 0.01.

slower uptake and processing mechanisms involved for the MHC class II processing of protein compared to SLPs (Figure 2.2B). The rapid and efficient processing of SLPs into MHC class I molecules was also observed with human DCs (Figure 2.2C). MoDCs loaded with SLPs activated CD8⁺ T cells already 1 h post-incubation. Ag presentation increased further with longer incubation periods and appeared to reach plateau levels at 3 h post-incubation. In line with the experiment shown in Figure 2.1A, no Ag presentation could be detected after incubation of MoDCs with GAG-protein, even when the concentration of the

protein was increased five-fold (data not shown). SSPs showed robust cytokine production, within 1 hour of Ag-loading. In general, the percentages of IFN- γ -producing CD8⁺ T cells stimulated by SLP-loaded DCs were lower compared to stimulation by DCs loaded with SSPs. GAG-protein could be cross-presented, however, if offered in an alternative way to APC. DCs loaded with protein fragments obtained by treatment with cyanogen bromide (CNBr) and Endo-Glu-C cross-presented the protein digest and activated HIV-specific CD8⁺ T cells, but with lower potency compared to SLP-GAG_{22aa} (Figure 2.2D). The CNBr and Endo-Glu-C generated GAG-protein digest was analyzed and yielded the specific fragments highlighted in Supporting Information Figure S2.1. HIV-specific CD8⁺ T cells readily recognized processed GAG-protein in its native conformation. DCs were incubated with NYVAC-C-infected apoptotic HeLa cells expressing among other viral proteins the GAG-protein⁵⁸, inducing potent activation of CD8⁺ T cells. DCs incubated with HeLa cells infected with NYVAC-WT (HIV GAG-negative) failed to activate HIV-specific CD8⁺ T cells. (Supporting Information Figure S2.2) Taken together, our data suggest that the method of Ag delivery is crucial for cross-presentation to be efficient and indicate that both murine and human DCs more efficiently internalize and process SLPs compared to soluble protein.

SLPs are primarily located outside endo-lysosomes upon internalization

To assess the internalization of SLPs by DCs, murine DCs were incubated for indicated time periods with fluorescently labeled SLP-OVA_{24aa}-Bodipy-FL (Figure 2.3A) or SLP-OVA_{17aa}-Bodipy-FL (Figure 2.3B) and the uptake was analyzed by confocal imaging. SLPs were internalized by DCs within 2 h of incubation. The fluorescence intensity increased with longer incubation, indicating continuous uptake of SLPs during 24 h. The integrity of the Bodipy-labeled SLPs was confirmed by analysis on Tricine-gel, excluding that Bodipy-dye was intracellularly cleaved from the SLPs resulting in free dye and SLP inside the cells (Supporting Information Figure S2.3). Next, the intracellular localization of SLPs and protein was compared. To this purpose, DCs were incubated with Ag and LysoTracker red and the co-localization between the Ag (green) and endo-lysosomes (red) was studied. Although SLPs is internalized within 2 h, we observed that DCs internalized SLP-OVA_{24aa}-Bodipy-FL and, the much slower endocytosed, OVA-protein-Alexa488 in sufficient amounts to be accurately detected and quantified after 24 h. The disparity in green fluorescence intensity is related to the intrinsic differences in the green dyes (1 Bodipy-FL dye per SLP molecule versus 4 – 5 Alexa488 dye's per protein molecule) used in the analysis. We have confirmed previously that Alexa488 and Bodipy-FL dyes do not differentially modulate

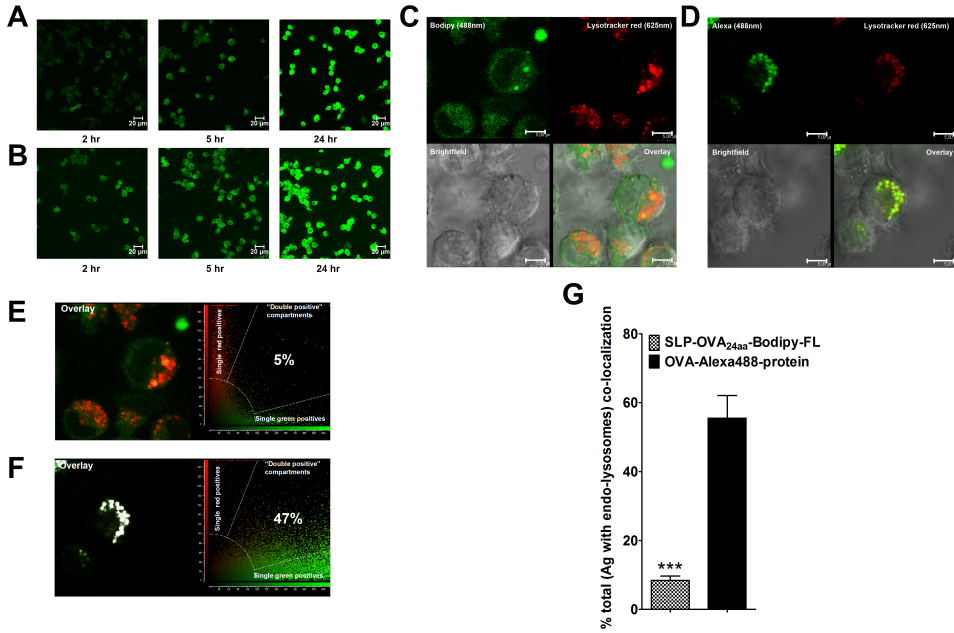


Figure 2.3 Distinct intracellular localization of SLPs and protein Ag in DCs.

DCs were incubated with 20 μ M **(A)** SLP-OVA_{24aa}-Bodipy-FL or **(B)** SLP-OVA_{17aa}-Bodipy-FL for 2, 5 and 24 h and analyzed by confocal microscopy (63x objective, scale bar, 20 μ m). **(C, D)** DCs loaded with 10 μ M SLP-OVA_{24aa}-Bodipy-FL or 10 μ M OVA-Alexa488-protein for 24 h were co-stained with LysoTracker red for visualization of endo-lysosomes. Confocal images of DCs incubated with **(C)** SLP-OVA_{24aa}-Bodipy-FL and **(D)** OVA-Alexa488 are shown as Bodipy/Alexa488/green fluorescence (top left), LysoTracker/red fluorescence (top right), bright field (bottom left) and overlay image (bottom right). **(C, D)** All scale bars, 5 μ m. **(E, F)** Co-localization of the green-fluorescence of **(E)** SLP-OVA_{24aa}-Bodipy-FL and **(F)** OVA-Alexa488 with endo-lysosomes was analyzed using Leica software (scatter plots) and **(G)** quantified results are depicted as mean + SEM of 10-20 samples from one experiment representative of two performed. Results are representative of four **(A, B)** or two **(C-G)** independent experiments analyzing 10-20 images per experiment. The Mann-Whitney test was applied to determine the difference between SLP-OVA_{24aa}-Bodipy-FL vs. OVA-Alexa488, ***P < 0.001.

uptake, intracellular routing and processing of Ag²². Internalized SLPs was detectable diffusely inside DCs (Figure 2.3C). The use of the lysoTracker red allowed the identification of distinct round (red fluorescent) organelles which represented endo-lysosomes. Upon overlay of the green and red fluorescent images, a low level of co-localization of the two colors was detected in DCs that were cultured with SLPs, indicating that SLPs was primarily outside the endo-lysosomes. In contrast, DCs which had internalized protein contained

distinct green-fluorescent hot spots within the cell which in addition had a high degree of co-localization with LysoTracker red resulting in a nearly complete absence of single red fluorescent compartments and appearance of yellow(ish) spots (Figure 2.3D). The results indicate that most, if not all, endo-lysosomes contained protein upon internalization by DCs. Co-localization was quantified by analyzing DCs which internalized SLPs (Figure 2.3E) or protein (Figure 2.3F). On average, in DCs cultured with SLPs, $8 \pm 3\%$ of the green signal detected co-localized with the red fluorescence detected. In comparison, in DCs loaded with protein (Figure 2.3F) as much as $56 \pm 18\%$ of the green signal detected co-localized with the red fluorescence (Figure 2.3G). In summary, after 24 h of Ag uptake, the majority of SLPs is localized outside of the endo-lysosomes whereas the majority of protein is present inside endo-lysosomes.

MHC class I Ag cross-presentation by DCs loaded with SLPs is proteasome- and TAP- dependent

The contribution of the proteasome, the transporter associated with Ag processing (TAP) and endosomal processing in the MHC class I cross-presentation of SLPs by DCs was investigated with SLP-OVA_{24aa} as model Ag. To this purpose, WT BMDCs were incubated with titrated amounts of SLPs (Figure 2.4A) or alternatively, the proteasome inhibitor epoxomicin was added during culture of DCs and SLPs (Figure 2.4B). We observed a nearly complete loss in MHC class I cross-presentation of SLPs when the proteasome function was inhibited, indicating that intracellular processing of SLPs is dependent on proteasome functionality. Epoxomicin-treated DCs cross-presented particulate forms of SLPs under similar conditions (Supporting Information Figure S2.4B), suggesting that the decrease of MHC class I cross-presentation via inhibition of the proteasome was mainly associated with the processing of soluble SLPs.

In comparison to WT BMDC, TAP1 KO BMDCs were largely deficient in activating CD8⁺T cells (Figure 2.4C). All DC conditions used to study MHC class I presentation of SLP efficiently presented SSP-OVA_{8aa} on MHC class I molecules indicating that epoxomicin or the absence of functional TAP did not affect the general MHC class I presentation machinery of DCs (Figure 2.4D). A potential role of endo-lysosomal acidification in the processing by DCs of SLPs was assessed by Ag-loading in the presence of titrated amounts of bafilomycin A (Baf A), a lysotropic reagent which inhibits acidification of endo-lysosomes thereby influencing the activity of pH-sensitive proteases present in these compartments. Only a moderate effect of Baf A on MHC class I cross-presentation was observed, reflected by

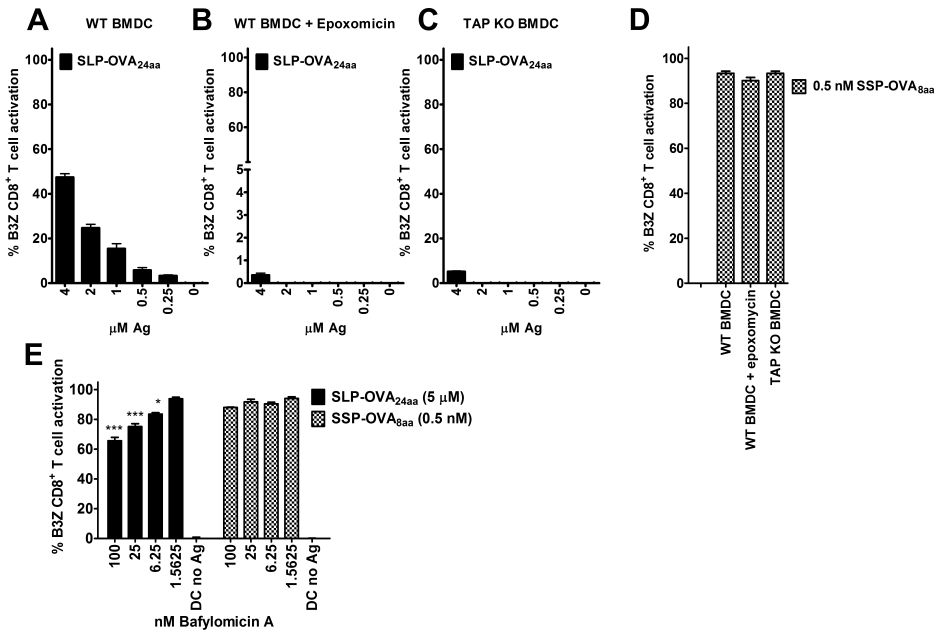


Figure 2.4 MHC class I Ag cross-presentation of SLPs depends on proteasome activity and TAP translocation.

WT C57BL/6 BMDCs were (A) left untreated or (B) pretreated for 60 min with 1 μM epoxomicin before culture with titrated amounts of SLP-OVA_{24aa} or (D) 0.5 nM SSP-OVA_{8aa}. (C, D) TAP1- KO BMDCs were loaded with titrated amounts of SLP-OVA_{24aa} or 0.5 nM SSP-OVA_{8aa}. (E) D1 cells were cultured with the indicated amounts of Baf A for 1 h and then loaded with 5 μM SLP-OVA_{24aa} and 0.5 nM SSP-OVA_{8aa} in continuous presence of Baf A. Ag incubation was carried out for 24 h, cells washed 3x times with complete medium and B3Z CD8⁺ T-cell activation determined after stimulation with Ag-loaded DCs. Data are shown as mean + SD of 3 samples from one experiment representative of three performed. (E) Statistical significance determined with two-way ANOVA and Bonferroni posttests, *** $P < 0.001$ & * $P < 0.05$.

a maximally 35% decrease in CD8⁺ T-cell activation at the highest concentration of the compound used (Figure 2.4E). DCs cross-presented SLPs with similar efficiency over a range of Ag-concentrations in the presence of Baf A comparable with that of untreated DCs whereas the cross-presentation of particulate SLPs was considerably decreased (Supporting Information Figure S2.4C, D and E). Lack of Cathepsin S did not modulate MHC class I cross-presentation of SLPs (Supporting Information 4C and E). Collectively, the results suggest that SLPs, upon internalization are most likely cross-presented into MHC class I molecules via classical cytosolic Ag presentation pathways.

SLPs are efficiently cross-presented by murine DCs but poorly by other cell types

Freshly isolated B and T cells were incubated with SLP-OVA_{24aa}, their MHC class I presentation capacity of SLPs compared to DCs. Maximum MHC class I presentation by the different cell types was based on the presentation of SSP-OVA_{8aa}. DCs (Figure 2.5A-C) were superior in cross-presentation of SLPs in comparison to B or T cells. Within this setting, B and T cells failed to activate CD8⁺ T cells upon loading with protein (data not shown). To better mimic the *in vivo* ratio of DC, B and T cells present in the draining lymph nodes (DLN)^{23,24}, MHC

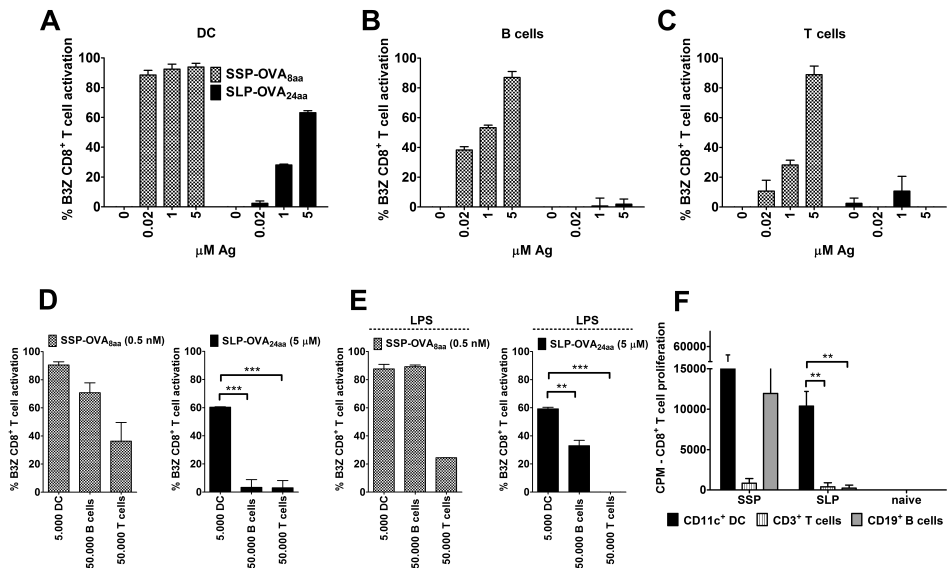


Figure 2.5 DCs specifically and more efficiently cross-present SLPs than B and T cells to CD8⁺ T cells.

(A-C) Five thousand (A) DCs, (B) B cells and (C) T cells were loaded with titrated amounts SLP-OVA_{24aa} and SSP-OVA_{8aa}. B and T-cell numbers were increased 10-fold (50,000 cells) and subsequently loaded with (D) 0.5 μM SSPs and 5 μM SLPs or with (E) LPS (10 μg/ml) added to the cultures. Ag incubation was carried out for 24 h, followed by washing steps and incubation with B3Z T cells. Mice were vaccinated with mixtures of 40 nmol SLP-OVA_{24aa} and 5 nmol CpG ODN 1826. 24 h after vaccination, animals were sacrificed, DLNs removed and CD11c⁺, CD19⁺ and CD3⁺ cells FACS-sorted out and used as APCs in a 72 h *ex vivo* culture with OT-I splenocytes. CD8⁺ OT-I proliferation was determined by ³H-thymidine incorporation. (A-E) Data are shown as mean + SD of 3 samples from one out of two independent cell isolations/experiments performed. (F) The averages ± SEM from two independent experiment/injections are shown. (D, E) Statistical significance determined with one-way ANOVA and Bonferroni posttests; (F) data compared using a Student's t-test. ***P < 0.001, **P < 0.01.

class I Ag presentation by 10-fold higher numbers of B and T cells were also compared to DCs. However, no improvement of CD8⁺ T-cell activation was observed (Figure 2.5D). LPS stimulation of B cells resulted in comparable presentation of SSPs to CD8⁺ T cells as by DCs, but DCs were still superior APC in cross-presenting SLPs even in the presence of LPS (Figure 2.5E). Finally, direct vaccinations with SLPs resulted in preferential internalization *in vivo* and presentation by DCs whereas SSPs can also be presented by B cells (Figure 2.5F). Collectively, these results point to DCs as the primary and most efficient APC to cross-present SLPs in MHC class I molecules.

Discussion

Using two distinct experimental Ag models, we show that both mouse and human DCs more efficiently cross-present SLPs in MHC class I molecules in contrast to whole protein Ag, which poorly induces MHC class I cross-presentation and under the conditions tested fails to activate CD8⁺ T cells. The improved MHC class I cross-presentation of SLPs is possibly related to the distinct intracellular localization of SLPs compared with that of protein Ag upon uptake by DCs. SLPs were shown to be located primarily outside the endo-lysosomes as early as 2 h after Ag incubation. The role of the proteasome and TAP next to the cytosolic presence suggest that SLP Ag is rapidly cross-presented into MHC class I molecules via the classical MHC class I Ag processing pathway^{25,26}, leading to efficient and potent activation of CD8⁺ T cells. Employing a faster cytosolic route upon internalization of SLPs, in contrast to the slower lysosomal route traveled by protein Ag^{27,28}, is compatible with the shorter time span needed for SLPs cross-presentation by DCs.

The advantages of substituting proteins or short peptides by SLPs in active immunization protocols, to enhance *in vivo* priming of anti-tumor CD4⁺ and CD8⁺ T cells have been shown and published before by our group²⁹ and also by others⁶. In these reports, mostly (pre-) clinical *in vivo* observations were described but not the processing mechanisms of SLPs by DCs and the efficiency of the ensuing MHC class I and class II presentation. We have now analyzed the mechanistic aspects of SLP processing and presentation by DCs and show in direct comparisons that SLPs facilitated MHC class I and II Ag presentation by DCs compared with that of equimolar concentrations of protein Ag. These results are in accordance with the study by Zhang et al.⁶ who showed that, in comparison to long peptide vaccines, vaccinations with soluble protein led to poor protection of mice against a lethal viral challenge which was associated with insufficient CD4⁺ T-cell responses and low specific CD8⁺ T-cell responses.

Relatively poor potency of protein based vaccines to induce CD8⁺ T-cell responses *in vitro* and *in vivo* can be enhanced by coupling of targeting moieties³⁰⁻³³ or via encapsulation in PLGA-particles³⁴. These methods are all believed to improve uptake and processing by professional APCs. Likewise, potency of SLPs can be further enhanced, via encapsulation in PLGA-particles³⁵, by antibody-targeting strategies³² and as published previously by our group, production of SLP-TLRL peptide-conjugates²² that will undergo phase I clinical trial testing in the near future.

Our data at face value might contradict other pre-clinical studies showing better MHC class I Ag presentation and CD8⁺ T-cell activation using OVA-protein as Ag²⁷. This discrepancy can be explained by the fact that the B3Z CD8⁺ T-cell clone used in our study to analyze MHC class I Ag presentation is co-stimulation independent and is purely dependent on the recognition of the H2-k^b/SIINFEKL complexes. Using co-stimulation dependent OT-I CD8⁺ T cells MHC class I cross-presentation of OVA was detected at concentrations starting from 0.0025 μM (data not shown) in accordance with other published reports³⁶. However, the use of co-stimulation-independent T-cell clones was vital in the current study to accurately analyze the efficiency of MHC-restricted Ag processing and presentation without interference by additional stimuli modulating T-cell activation.

In the human model, no MHC class I cross-priming of HIV-specific CD8⁺ T cells was detected using whole soluble GAG-protein. MHC class I presentation could be induced by loading DCs with pre-cleaved protein fragments. This observation suggests that the intracellular processing of internalized whole soluble GAG-protein is very inefficient and that pre-cleaved protein fragments facilitate internalization and intracellular Ag processing.

SLPs were clearly present inside DCs after 2 h of incubation. Previous work by our group revealed that DCs required more than 30 min to internalize the SLPs²². As observed before, internalized soluble intact protein ended up mainly in the endosomes of DCs^{37,38}, whereas most of the internalized SLPs was localized outside the endo-lysosomal compartments at all the time points analyzed. Our results partially differ from an earlier published study reporting a larger fraction of internalized long peptides inside the lysosomes. In this study internalized long peptides were detected outside lysosomes at early- but not at late time points⁶. In addition, the authors reported dotted patterns of long peptide Ag inside DCs in contrast to the diffuse pattern of internalized SLPs, mainly located outside the endo-lysosomes, as we show here. These differences might be related to the DCs used in the respective studies with possibly different functional properties. Zhang et al. used the

DC2.4 murine bone marrow-derived DCs cell line³⁹. We used D1 cells, a cell line closely resembling primary DCs⁴⁰. Confocal analysis with freshly cultured BMDCs confirmed that internalized SLPs were present throughout the cell (data not shown). Importantly, both our results and those of Zhang et al.⁶ show that protein Ag does not or poorly access the cytosol upon internalization by DCs. Therefore, we can conclude that (synthetic) long peptide Ag and protein Ag are routed differently in DCs.

Lack of specific markers for the cytosol thwarted our attempts to conclusively show that SLPs are in the cytosol. Nevertheless, the proteasome inhibition experiments and experiments with TAP1 KO DCs provide important evidence that ingested SLPs end up in the cytosol for processing and presentation.

Some recent reports have indicated that some proteases associated with MHC class II Ag presentation could also play a role in class I cross-presentation^{25,26}. Ag trimming in endo-lysosomes by proteases are pH-dependent. A significant role for Cathepsin S, which has optimal activity at neutral pH⁴¹, in the processing of SLPs into MHC class I molecules was excluded. Inhibitors of endo-lysosomal acidification have been shown to block the translocation of protein from the endosomes to the cytosol⁴². The minor decrease in MHC class I presentation of SLPs by DCs in the presence of Baf A might be due to decreased translocation of internalized SLPs from the endo-lysosomes to the cytosol, limiting the amount of SLPs cleaved by the proteasome..

DCs incubated with SSPs resulted in the most rapid and vigorous T-cell activation in comparison to the SLPs. However, immunizations with SSPs are associated with considerable limitations^{43,44}; for example the lack of CD4⁺ T-cell help characterizing the use of short peptides representing minimal CD8⁺ T-cell epitopes. Other restrictions are the necessity for HLA-typing for each patient to be treated and tolerance induction due to SSP presentation by non-professional APC¹¹. Another disadvantage of SSPs is the short-lived *in vitro* Ag presentation in comparison to SLPs⁴⁵ which, next to SSP loading on non-professional APCs might underlie the vanishing CD8⁺ T-cell responses observed *in vivo* following vaccination with SSPs⁴⁶. SLPs are not able to bind directly to MHC class I and their presentation to CD8⁺ T cells therefore requires uptake and processing by DCs before they are presented^{43,47}. Interestingly, Eikawa et al showed that MHC class I presentation by human APC of NY-ESO-1 long peptides could be blocked by inhibiting actin filament formation⁴⁷.

A vital aspect of efficient T-cell priming *in vivo* is specific Ag presentation by DCs and not by other immune cells that lack the capacity to provide adequate co-stimulation and thus

may cause T-cell tolerance^{48,49}. DCs are present in lower numbers in human blood but also in lymphoid tissues^{23,24}. In addition, s.c. or intradermally administered SLP-vaccines do not require active transport by phagocytic cells due to their small size (1.5 – 5 kD). Most likely SLP-vaccines enter the DLN through passive transport⁵⁰ where they encounter abundant numbers of B cells in the B-cell follicles before accessing resident or migrating DCs present in the T-cell zone^{51,52}. But B cells isolated from vaccinated animals were not capable of priming naïve CD8⁺ T cells *ex vivo* 1 day post subcutaneous vaccination with SLPs (Figure 2.5), whereas CD11c⁺ DCs isolated from the same DLN showed potent capacity to prime naïve CD8⁺ T cells. in accordance with the data of Bijker et al.⁸.

Previous reports describing the *in vivo* potency of vaccinations with SLPs have not revealed a mechanistic basis for the observed enhanced anti-tumor T-cell responses in cancer patients^{9,53}.

Our novel findings, involving a head to head comparison show conclusively that SLPs are far more efficiently processed into both the MHC class I and class II Ag presentation pathways by DCs in comparison with soluble protein. MHC class I cross-presentation of SLPs is accomplished via processing mechanisms most commonly associated with the classical cytosolic MHC class I Ag cross-presentation pathways⁵⁴. In addition, DCs loaded with SLPs potently activate CD4⁺ T cells. Dual priming of both CD4⁺ and CD8⁺ T cells by the same DCs likely underlies the potent and efficient adaptive cellular immune responses observed upon therapeutic vaccinations with SLPs in patients with (pre-)malignant diseases.

Material and methods

Mice

WT C57BL/6 (CD45.2/Thy1.2; H2-K^b) mice were obtained from Charles River Laboratories (France). F1 progeny of C57BL/6 x C3H (H2-K^k) and OT-I/Thy1.1/CD45.2 were bred in the specific pathogen-free animal facility of the Leiden University Medical Center. TAP1 KO mice (C57BL/6 CD45.2/Thy1.2; H2-K^b) were purchased from the Jackson laboratory (Bar Harbor, ME). All mice were used at 8–12 weeks of age in accordance with national legislation and under supervision of the animal experimental committee of the University of Leiden.

Peptides and proteins

For the murine OVA-experimental model, peptides were generated, purified, dissolved and stored as described previously⁵⁵. Fluorescent labeling of SLP-OVA_{24aa} with BODIPY-FL N-(2-aminoethyl) maleimide was performed as described before (Table 2.1)⁵⁵ and endotoxin-free ovalbumin (OVA, Worthington LS003048) used. Ovalbumin-Alexa Fluor® 488 was purchased from Invitrogen. Table 2.1 also describes the peptides used for the experiments with human cells. HIV-1 GAG-protein was generated as described before⁵⁶, over-expressed in Escherichia coli BL21 (DE3) and purified as described before⁵⁷.

Cells

Human monocyte derived DC (MoDC) were obtained from freshly isolated peripheral blood mononuclear cells (PBMCs) in buffy coats of healthy blood donors and generated by isolating CD14⁺ monocytes. The generation of the HIV-specific CD8⁺ T-cell line has been

Table 2.1 List of peptides used

Abbreviation	Location in protein (begin-end)	Chemical modifications	Sequence
SSP-OV _{A8a}	257–264	SSP-OVA _{257–264}	<u>SIINFEKL</u>
SSP-OVA _{8aa}	257–264	SSP-OVA _{257–264} -Bodipy	<u>SIINFEKL</u> -Bodipy
SLP-OV _{A24a}	247–264	SLP-OVA _{247–264} ASK	DEVSGLEQLES <u>SIINFEKL</u> AAAAAK
SLP-OVA _{24aa} -Bodipy	247–264	SLP-OVA _{247–264} ASK-Bodipy	DEVSGLEQLES <u>SIINFEKL</u> AAAAAK-Bodipy
SLP-OVA _{31aa}	240–264	SLP-OVA _{240–264} ASK	SMLVLLPDEVSGLEQLES <u>SIINFEKL</u> AAAAAK
SLP-OVA _{31aa} -Bodipy	240–264	SLP-OVA _{240–264} ASK-Bodipy	SMLVLLPDEVSGLEQLES <u>SIINFEKL</u> AAAAAK-Bodipy
SLP-OVA _{17aa}	323–339	SLP-OVA _{323–339}	<u>ISQAVHAAHAEINEAGR</u>
SLP-OVA _{17aa} -Bodipy	323–339	SLP-OVA _{323–339} -Bodipy	<u>ISQAVHAAHAEINEAGR</u> -Bodipy
SLP-OVA _{31aa}	316–346	SLP-OVA _{316–346}	SSAESLK <u>ISQAVHAAHAEINEAGRE</u> VVGS
SLP-OVA _{31aa} -Bodipy	316–346	SLP-OVA _{316–346} -Bodipy	SSAESLK <u>ISQAVHAAHAEINEAGRE</u> VVGS
SSP-GA _{G9a}	223–231	SSP-GAG _{223–231}	<u>GPGHKARVL</u>
SLP-GA _{G22a}	216–237	SLP-GAG _{216–237}	TACQGVGG <u>GPGHKARVL</u> AEAMSQ

described before⁵⁸. Freshly isolated murine DC were cultured from mouse bone marrow (BM) cells, as described before⁵⁹. The D1 cell line, an immature primary splenic DC line (C57BL/6-derived), was cultured as described elsewhere⁶⁰. B3Z CD8⁺ T cells, OT-IIZ and KZO CD4⁺ T-cells are hybridoma cell lines expressing a β -galactosidase construct which upon T-cell activation can be measured by a colorimetric assay²².

Murine MHC class I and class II Ag presentation assays

Unless otherwise indicated, 100,000 DC were plated out in triplicate using Greiner flat bottom 96-wells plate (#655101) and incubated for 24 hr with the Ags at the indicated concentrations. In some experiments, DCs were cultured in the presence of 10 μ g/ml LPS prior to Ag incubation. Cells were washed 3x times with complete medium to remove excess Ag before the T-cell hybridoma B3Z CD8⁺ T cells (H2-k^b/SIINFEKL), KZO CD4⁺ T cells (I-A^k/DEVSGLEQLESI) or OT-IIZ CD4⁺ T cells (I-A^{kb}/ISQAVHAAHAEINEAGR) were added. T cells were cultures in the presence of Ag-loaded DC O/N at 37°C. To study kinetics of MHC class I and class II presentation, DCs were incubated with 10 nM SSPs, 10 μ M SLPs or 10 μ M protein for 1, 3 or 5 hr. After 3x washing, DCs were fixated by adding 50 μ l/well of 0.2% PFA for 15 min. Fixation was blocked by adding 150 μ l/well complete medium. In experiments aimed to study intracellular processing pathways involved in SLP-cross presentation in MHC class I molecules, BMDC or D1 cells were pre-incubated with epoxomicin (324800, Merck) or bafilomycin A1 (196000, Merck) followed by Ag-incubation as described above in the presence of the compounds. To assess Ag presentation by other cells in comparison to DC, B and T cells were isolated from total spleen single cell suspensions, FACS-sorted, and incubated with titrated amounts of SLP-OVA_{24aa'}, SSP-OVA_{8aa} or OVA and subsequently used as APC in co-cultures with B3Z CD8⁺ T cells as described above.

***In vitro* analysis of human T-cell activation**

Human CD8⁺ T-cell activation was studied using MoDC cross-presenting Ags to human HIV-specific CD8 T cells. The cytokine production of HIV-specific CD8⁺ T cells was used as read out. To this purpose, MoDC were incubated for the indicated time with Gag-protein, SLP-GAG_{22aa'}, SSP-GAG_{9aa} or medium as a control. After the indicated incubation, MoDC were fixed with 0.2% paraformaldehyde (PFA) to prevent further processing and HIV-specific CD8 T cells were added (at approximately 5 T-cell: 1 DC ratio) followed by

overnight culture at 37°C/5%CO₂. After 18 hr, supernatant was harvested to determine IFN-γ production by ELISA according to the manufacturer's protocol (Sanquin, Amsterdam, The Netherlands).

***In vitro* analysis of human T-cell activation by MoDC incubated with Endo-Gluc-CNBr GAG-protein fragments**

Human CD8⁺ T-cell activation was studied using MoDC cross-presenting EndoGluc-CNBr GAG-protein fragments, which were generated as described above, to human HIV-specific CD8 T cells. The cytokine production of HIV-specific CD8⁺ T cells was used as read out. For this purpose, MoDC were incubated with GAG-protein, SLP-GAG_{22aa} and EndoGluc-CNBr GAG-protein fragments. After 24 hr incubation, HIV-specific CD8 T-cells were added (at approximately 5 T-cell: 1 DC ratio) followed by overnight culture at 37°C/5%CO₂. Brefeldin A (10 μg/ml, Sigma-Aldrich) was added to retain cytokines within the T-cells allowing the detection of multiple cytokines. After 18 hr, intracellular cytokine staining (ICS) was performed as described⁶¹. Cells were fixed and permeabilized using Cytofix/Cytoperm™ Fixation/Permeabilization Solution Kit (BD). Cells were then incubated with α-TNF PE-Cy7 (clone MAb11, eBiosciences), α-IFN-γ FITC, α-IL-2 APC, α-MIP-1β PE (all three from BD) and α-CD8 PerCP (Dako). After washing, cells were analyzed by flow cytometry using a LSRII flow cytometer (BD Pharmingen) and analyzed with FlowJo software (Treestar). Cells were first gated based on the characteristics forward and side scatter properties, followed by identification of CD3⁺CD8⁺ T cells followed by intracellular analysis of cytokines produced within the gated CD8⁺ T cells. Net accumulation of activated GAG-specific CD8⁺ T-cells is the percentage of live CD8⁺ cells expressing one or more of the analyzed cytokines upon stimulation with MoDC loaded with Ag.

Confocal microscopy

DC were incubated for 2, 5 and 24 hr with 20 μM SLP-OVA_{17aa}-Bodipy and SLP-OVA_{24aa}-Bodipy at 37°C. After incubation cells were washed 3 times to remove excess and unbound Ag, resuspended at a concentration of 2x10⁵ cells in 200 μl complete medium and plated into poly-d-lysine coated glass-bottom dishes (MatTek) followed by mild centrifugation to allow the cells to adhere. Adhered cells were then fixed with 0.2% paraformaldehyde. All experiments were carried out on a Leica TCS SP5 confocal microscope (HCX PL APO 63x/1.4 NA oil-immersion objective, 12 bit resolution, 1024x1024 pixels, pinhole 2.1 Airy

discs, zoomfactor 1 or 7). Imaging was performed using the 488 nm line from an Argon laser collecting emission between 500 and 600 nm.

Alternatively, DC were incubated for 24 hr with 10 μ M OVA-protein-Alexa488 or SLP-OVA_{24aa}-Bodipy at 37°C. After incubation cells were washed 3 times to remove excess and unbound Ag followed by 30 min incubation with 300 nM LysoTracker® red (Invitrogen) to stain endo-lysosomal compartments. After incubation, cells were washed and resuspended at a concentration of 2×10^5 cells 200 μ l and plated into poly-d-lysine coated glass-bottom dishes (MatTek) 2 hr before analysis to allow cells to adhere. Cells were imaged using an inverted Leica TCS SP5 confocal microscope. Dual color images were acquired by sequential scanning, with only one laser per scan to avoid cross talk. The images were analyzed using the Leica software program (LAS AF).

Vaccination and *ex vivo* Ag presentation

Animals were injected subcutaneously (s.c.) with 40 nmol of SLPs or SSPs mixed with 5 nmol CpG (Invivogen). One day later, sacrificed and draining lymph nodes (DLN) harvested and single cell suspensions prepared. To assess *ex vivo* Ag presentation, CD11c⁺ DC, CD19⁺ B and CD3⁺ T cells were isolated purified using FACS-sorting from DLN cell suspensions and subsequently used as APC in co-cultures with OT-I CD8⁺ T cells.

Statistics

Statistical analyses applied to determine the significance of differences are described in the figure legends.

Acknowledgements

We acknowledge the support of Ing. A. van der Laan from the Dept of Molecular Cell biology and Imaging Facility of the LUMC. We thank Dr. Nilabh Shastri for his kind gift of the KZO T-cell hybridoma. The following reagent was obtained through the NIH AIDS Research and Reference Reagent Program, Division of AIDS, NIAID, NIH: pGag-EGFP (Cat#11468) from Dr. Marilyn Resh. The PBMCs from which the HIV-specific CD8⁺ T cells were generated were kindly provided by Prof. G. Pantaleo. This study was supported by grants from Immune System Activation (ISA) Pharmaceuticals, University of Leiden and the Leiden University Medical Center.

References

1. Banchereau J, Steinman RM 1998. Dendritic cells and the control of immunity. *Nature* 392:245-252.
2. Huang LM, Lu CY, Chen DS 2011. Hepatitis B virus infection, its sequelae, and prevention by vaccination. *Curr Opin Immunol* 23:237-243.
3. Frazer IH, Lowy DR, Schiller JT 2007. Prevention of cancer through immunization: Prospects and challenges for the 21st century. *Eur J Immunol* 37 Suppl 1:S148-S155.
4. Schiller JT, Lowy DR 2010. Vaccines to prevent infections by oncoviruses. *Annu Rev Microbiol* 64:23-41.
5. Atanackovic D, Altorki NK, Stockert E, Williamson B, Jungbluth AA, Ritter E, Santiago D, Ferrara CA, Matsuo M, Selvakumar A, Dupont B, Chen YT, Hoffman EW, Ritter G, Old LJ, Gnjjatic S 2004. Vaccine-induced CD4+ T cell responses to MAGE-3 protein in lung cancer patients. *J Immunol* 172:3289-3296.
6. Zhang H, Hong H, Li D, Ma S, Di Y, Stoten A, Haig N, Di GK, Yu Z, Xu XN, McMichael A, Jiang S 2009. Comparing pooled peptides with intact protein for accessing cross-presentation pathways for protective CD8+ and CD4+ T cells. *J Biol Chem* 284:9184-9191.
7. Chua BY, Pejoski D, Turner SJ, Zeng W, Jackson DC 2011. Soluble proteins induce strong CD8+ T cell and antibody responses through electrostatic association with simple cationic or anionic lipopeptides that target TLR2. *J Immunol* 187:1692-1701.
8. Bijker MS, van den Eeden SJ, Franken KL, Melief CJ, van der Burg SH, Offringa R 2008. Superior induction of anti-tumor CTL immunity by extended peptide vaccines involves prolonged, DC-focused antigen presentation. *Eur J Immunol* 38:1033-1042.
9. Kenter GG, Welters MJ, Valentijn AR, Lowik MJ, Berends-van der Meer DM, Vloon AP, Essahsah F, Fathers LM, Offringa R, Drijfhout JW, Wafelman AR, Oostendorp J, Fleuren GJ, van der Burg SH, Melief CJ 2009. Vaccination against HPV-16 oncoproteins for vulvar intraepithelial neoplasia. *N Engl J Med* 361:1838-1847.
10. Kenter GG, Welters MJ, Valentijn AR, Lowik MJ, Berends-van der Meer DM, Vloon AP, Drijfhout JW, Wafelman AR, Oostendorp J, Fleuren GJ, Offringa R, van der Burg SH, Melief CJ 2008. Phase I immunotherapeutic trial with long peptides spanning the E6 and E7 sequences of high-risk human papillomavirus 16 in end-stage cervical cancer patients shows low toxicity and robust immunogenicity. *Clin Cancer Res* 14:169-177.
11. Melief CJ, van der Burg SH 2008. Immunotherapy of established (pre)malignant disease by synthetic long peptide vaccines. *Nat Rev Cancer* 8:351-360.
12. Welters MJ, Kenter GG, de Vos van Steenwijk PJ, Lowik MJ, Berends-van der Meer DM, Essahsah F, Stynenbosch LF, Vloon AP, Ramwadhoebe TH, Piersma SJ, van der Hulst JM, Valentijn AR, Fathers LM, Drijfhout JW, Franken KL, Oostendorp J, Fleuren GJ, Melief CJ, van der Burg SH 2010. Success or failure of vaccination for HPV16-positive vulvar lesions correlates with kinetics and phenotype of induced T-cell responses. *Proc Natl Acad Sci U S A* 107:11895-11899.

13. Speetjens FM, Kuppen PJ, Welters MJ, Essahsah F, Voet van den Brink AM, Lantrua MG, Valentijn AR, Oostendorp J, Fathers LM, Nijman HW, Drijfhout JW, van d, V, Melief CJ, van der Burg SH 2009. Induction of p53-specific immunity by a p53 synthetic long peptide vaccine in patients treated for metastatic colorectal cancer. *Clin Cancer Res* 15:1086-1095.
14. Sabbatini P, Tsuji T, Ferran L, Ritter E, Sedrak C, Tuballes K, Jungbluth AA, Ritter G, Aghajanian C, Bell-McGuinn K, Hensley ML, Konner J, Tew W, Spriggs DR, Hoffman EW, Venhaus R, Pan L, Salazar AM, Diefenbach CM, Old LJ, Gnjjatic S 2012. Phase I Trial of Overlapping Long Peptides from a Tumor Self-Antigen and Poly-ICLC Shows Rapid Induction of Integrated Immune Response in Ovarian Cancer Patients. *Clinical Cancer Research* 18:6497-6508.
15. Arevalo-Herrera M, Soto L, Perlaza BL, Cespedes N, Vera O, Lenis AM, Bonelo A, Corradin G, Herrera S 2011. Antibody-mediated and cellular immune responses induced in naive volunteers by vaccination with long synthetic peptides derived from the Plasmodium vivax circumsporozoite protein. *Am J Trop Med Hyg* 84:35-42.
16. Olugbile S, Villard V, Bertholet S, Jafarshad A, Kulangara C, Roussillon C, Frank G, Agak GW, Felger I, Nebie I, Konate K, Kajava AV, Schuck P, Druilhe P, Spertini F, Corradin G 2011. Malaria vaccine candidate: Design of a multivalent subunit alpha-helical coiled coil poly-epitope. *Vaccine* 29:7090-7099.
17. Rosario M, Bridgeman A, Quakkelaar ED, Quigley MF, Hill BJ, Knudsen ML, Ammendola V, Ljungberg K, Borthwick N, Im EJ, McMichael AJ, Drijfhout JW, Greenaway HY, Venturi V, Douek DC, Colloca S, Liljestrom P, Nicosia A, Price DA, Melief CJ, Hanke T 2010. Long peptides induce polyfunctional T cells against conserved regions of HIV-1 with superior breadth to single-gene vaccines in macaques. *Eur J Immunol* 40:1973-1984.
18. Rosario M, Borthwick N, Stewart-Jones GB, Mbewe-Mvula A, Bridgeman A, Colloca S, Montefiori D, McMichael AJ, Nicosia A, Quakkelaar ED, Drijfhout JW, Melief CJ, Hanke T 2012. Prime-boost regimens with adjuvanted synthetic long peptides elicit T cells and antibodies to conserved regions of HIV-1 in macaques. *AIDS* 26:275-284.
19. Zeng G, Li Y, El-Gamil M, Sidney J, Sette A, Wang Rf, Rosenberg SA, Robbins PF 2002. Generation of NY-ESO-1-specific CD4+ and CD8+ T Cells by a Single Peptide with Dual MHC Class I and Class II Specificities. *Cancer Research* 62:3630-3635.
20. Knutson KL, Schiffman K, Disis ML 2001. Immunization with a HER-2/neu helper peptide vaccine generates HER-2/neu CD8 T-cell immunity in cancer patients. *J Clin Invest* 107:477-484.
21. van der Burg SH, Melief CJ 2011. Therapeutic vaccination against human papilloma virus induced malignancies. *Curr Opin Immunol* 23:252-257.
22. Khan S, Bijker MS, Weterings JJ, Tanke HJ, Adema GJ, van HT, Drijfhout JW, Melief CJ, Overkleef HS, van der Marel GA, Filippov DV, van der Burg SH, Ossendorp F 2007. Distinct uptake mechanisms but similar intracellular processing of two different toll-like receptor ligand-peptide conjugates in dendritic cells. *J Biol Chem* 282:21145-21159.
23. Baldazzi V, Paci P, Bernaschi M, Castiglione F 2009. Modeling lymphocyte homing and encounters in lymph nodes. *BMC Bioinformatics* 10:387.

24. von Andrian UH, Mempel TR 2003. Homing and cellular traffic in lymph nodes. *Nat Rev Immunol* 3:867-878.
25. Singh R, Cresswell P 2010. Defective cross-presentation of viral antigens in GILT-free mice. *Science* 328:1394-1398.
26. Rock KL, Farfan-Arribas DJ, Shen L 2010. Proteases in MHC class I presentation and cross-presentation. *J Immunol* 184:9-15.
27. Burgdorf S, Scholz C, Kautz A, Tampe R, Kurts C 2008. Spatial and mechanistic separation of cross-presentation and endogenous antigen presentation. *Nat Immunol* 9:558-566.
28. Chen L, Jondal M 2004. Endolysosomal processing of exogenous antigen into major histocompatibility complex class I-binding peptides. *Scand J Immunol* 59:545-552.
29. Zwaveling S, Ferreira Mota SC, Nouta J, Johnson M, Lipford GB, Offringa R, van der Burg SH, Melief CJ 2002. Established human papillomavirus type 16-expressing tumors are effectively eradicated following vaccination with long peptides. *J Immunol* 169:350-358.
30. Bonifaz LC, Bonnyay DP, Charalambous A, Darguste DI, Fujii S, Soares H, Brimnes MK, Moltedo B, Moran TM, Steinman RM 2004. In vivo targeting of antigens to maturing dendritic cells via the DEC-205 receptor improves T cell vaccination. *J Exp Med* 199:815-824.
31. Rudd BD, Brien JD, Davenport MP, Nikolich-Zugich J 2008. Cutting edge: TLR ligands increase TCR triggering by slowing peptide-MHC class I decay rates. *J Immunol* 181:5199-5203.
32. Kreutz M, Giquel B, Hu Q, Abuknesha R, Uematsu S, Akira S, Nestle FO, Diebold SS 2012. Antibody-antigen-adjuvant conjugates enable co-delivery of antigen and adjuvant to dendritic cells in cis but only have partial targeting specificity. *PLoS One* 7:e40208.
33. Singh SK, Streng-Ouwehand I, Litjens M, Kalay H, Burgdorf S, Saeland E, Kurts C, Unger WW, van KY 2011. Design of neo-glycoconjugates that target the mannose receptor and enhance TLR-independent cross-presentation and Th1 polarization. *Eur J Immunol* 41:916-925.
34. Shen H, Ackerman AL, Cody V, Giodini A, Hinson ER, Cresswell P, Edelson RL, Saltzman WM, Hanlon DJ 2006. Enhanced and prolonged cross-presentation following endosomal escape of exogenous antigens encapsulated in biodegradable nanoparticles. *Immunology* 117:78-88.
35. Silva AL, Rosalia RA, Sazak A, Carstens MG, Ossendorp F, Oostendorp J, Jiskoot W Optimization of encapsulation of a synthetic long peptide in PLGA nanoparticles: low burst release is crucial for efficient CD8+ T cell activation. *European Journal of Pharmaceutics and Biopharmaceutics*.
36. Burgdorf S, Schuette V, Semmling V, Hochheiser K, Lukacs-Kornek V, Knolle PA, Kurts C 2010. Steady-state cross-presentation of OVA is mannose receptor-dependent but inhibitable by collagen fragments. *Proc Natl Acad Sci U S A* 107:E48-E49.
37. Chen L, Jondal M 2004. Endolysosomal processing of exogenous antigen into major histocompatibility complex class I-binding peptides. *Scand J Immunol* 59:545-552.
38. Burgdorf S, Scholz C, Kautz A, Tampe R, Kurts C 2008. Spatial and mechanistic separation of cross-presentation and endogenous antigen presentation. *Nat Immunol* 9:558-566.

39. Hargadon KM, Forrest OA, Reddy PR 2012. Suppression of the maturation and activation of the dendritic cell line DC2.4 by melanoma-derived factors. *Cellular Immunology* 272:275-282.
40. van Helden SFG, van Leeuwen FN, Figdor CG 2008. Human and murine model cell lines for dendritic cell biology evaluated. *Immunology Letters* 117:191-197.
41. Claus V, Jahraus A, Tjelle T, Berg T, Kirschke H, Faulstich H, Griffiths G 1998. Lysosomal enzyme trafficking between phagosomes, endosomes, and lysosomes in J774 macrophages. Enrichment of cathepsin H in early endosomes. *J Biol Chem* 273:9842-9851.
42. Horiguchi M, Arita M, Kaempf-Rotzoll DE, Tsujimoto M, Inoue K, Arai H 2003. pH-dependent translocation of alpha-tocopherol transfer protein (alpha-TTP) between hepatic cytosol and late endosomes. *Genes Cells* 8:789-800.
43. Melief CJ 2008. Cancer immunotherapy by dendritic cells. *Immunity* 29:372-383.
44. van HT, van der Burg SH 2012. Mechanisms of peptide vaccination in mouse models: tolerance, immunity, and hyperreactivity. *Adv Immunol* 114:51-76.
45. Faure F, Mantegazza A, Sadaka C, Sedlik C, Jotereau F, Amigorena S 2009. Long-lasting cross-presentation of tumor antigen in human DC. *Eur J Immunol* 39:380-390.
46. Bijker MS, van den Eeden SJ, Franken KL, Melief CJ, Offringa R, van der Burg SH 2007. CD8+ CTL priming by exact peptide epitopes in incomplete Freund's adjuvant induces a vanishing CTL response, whereas long peptides induce sustained CTL reactivity. *J Immunol* 179:5033-5040.
47. Eikawa S, Kakimi K, Isobe M, Kuzushima K, Luescher I, Ohue Y, Ikeuchi K, Uenaka A, Nishikawa H, Uono H, Oka M, Nakayama E 2013. Induction of CD8 T-cell responses restricted to multiple HLA class I alleles in a cancer patient by immunization with a 20-mer NY-ESO-1f (NY-ESO-1 91-110) peptide. *Int J Cancer* 132:345-354.
48. Guermonprez P, Valladeau J, Zitvogel L, Thery C, Amigorena S 2002. Antigen presentation and T cell stimulation by dendritic cells. *Annu Rev Immunol* 20:621-667.
49. Bennett SR, Carbone FR, Toy T, Miller JF, Heath WR 1998. B cells directly tolerize CD8(+) T cells. *J Exp Med* 188:1977-1983.
50. Manolova V, Flace A, Bauer M, Schwarz K, Saudan P, Bachmann MF 2008. Nanoparticles target distinct dendritic cell populations according to their size. *Eur J Immunol* 38:1404-1413.
51. Jenkins MK, Khoruts A, Ingulli E, Mueller DL, McSorley SJ, Reinhardt RL, Itano A, Pape KA 2001. In vivo activation of antigen-specific CD4 T cells. *Annu Rev Immunol* 19:23-45.
52. Gretz JE, Norbury CC, Anderson AO, Proudfoot AE, Shaw S 2000. Lymph-borne chemokines and other low molecular weight molecules reach high endothelial venules via specialized conduits while a functional barrier limits access to the lymphocyte microenvironments in lymph node cortex. *J Exp Med* 192:1425-1440.

53. de Vos van Steenwijk PJ, Ramwadhoebe TH, Lowik MJ, van der Minne CE, Berends-van der Meer DM, Fathers LM, Valentijn AR, Oostendorp J, Fleuren GJ, Hellebrekers BW, Welters MJ, van Poelgeest MI, Melief CJ, Kenter GG, van der Burg SH 2012. A placebo-controlled randomized HPV16 synthetic long-peptide vaccination study in women with high-grade cervical squamous intraepithelial lesions. *Cancer Immunol Immunother* 61:1485-1492.
54. Joffre OP, Segura E, Savina A, Amigorena S 2012. Cross-presentation by dendritic cells. *Nat Rev Immunol* 12:557-569.
55. Feltkamp MC, Smits HL, Vierboom MP, Minnaar RP, de Jongh BM, Drijfhout JW, ter Schegget J, Melief CJ, Kast WM 1993. Vaccination with cytotoxic T lymphocyte epitope-containing peptide protects against a tumor induced by human papillomavirus type 16-transformed cells. *Eur J Immunol* 23:2242-2249.
56. Schwartz S, Campbell M, Nasioulas G, Harrison J, Felber BK, Pavlakis GN 1992. Mutational inactivation of an inhibitory sequence in human immunodeficiency virus type 1 results in Rev-independent gag expression. *Journal of Virology* 66:7176-7182.
57. Franken KL, Hiemstra HS, van Meijgaarden KE, Subronto Y, den Hartigh J, Ottenhoff TH, Drijfhout JW 2000. Purification of his-tagged proteins by immobilized chelate affinity chromatography: the benefits from the use of organic solvent. *Protein Expr Purif* 18:95-99.
58. Quakkelaar ED, Redeker A, Haddad EK, Harari A, McCaughey SM, Duhon T, Filali-Mouhim A, Goulet JP, Loof NM, Ossendorp F, Perdiguero B, Heinen P, Gomez CE, Kibler KV, Koelle DM, Sekaly RP, Sallusto F, Lanzavecchia A, Pantaleo G, Esteban M, Tartaglia J, Jacobs BL, Melief CJ 2011. Improved innate and adaptive immunostimulation by genetically modified HIV-1 protein expressing NYVAC vectors. *PLoS One* 6:e16819.
59. van Montfoort N, Camps MG, Khan S, Filippov DV, Weterings JJ, Griffith JM, Geuze HJ, van Hall T, Verbeek JS, Melief CJ, Ossendorp F 2009. Antigen storage compartments in mature dendritic cells facilitate prolonged cytotoxic T lymphocyte cross-priming capacity. *Proc Natl Acad Sci U S A* 106:6730-6735.
60. Schuurhuis DH, Ioan-Facsinay A, Nagelkerken B, van Schip JJ, Sedlik C, Melief CJ, Verbeek JS, Ossendorp F 2002. Antigen-antibody immune complexes empower dendritic cells to efficiently prime specific CD8+ CTL responses in vivo. *J Immunol* 168:2240-2246.
61. Jing L, McCaughey SM, Davies DH, Chong TM, Felgner PL, De Rosa SC, Wilson CB, Koelle DM 2009. ORFeome approach to the clonal, HLA allele-specific CD4 T-cell response to a complex pathogen in humans. *J Immunol Methods* 347:36-45.

Supporting Information – Material and methods

HIV-1 GAG-protein Identification by Mass Spectrometry (MS)

HIV-GAG protein was digested with CNBr and endoproteinase GluC as follows: 400 µg HIV-GAG was reduced with DTT and alkylated with iodoacetamide. Chemical cleavage at methionine with CNBr in 70% formic acid was performed as described by ¹. After lyophilization, the protein was additionally digested for 16 h at ambient temperature with 40 µg endoproteinase GluC (Worthington) in ammonium bicarbonate pH 7.8. The mixture was passed through a 30 kD Microcon (Millipore) filter and peptides recovered from the filtrate (flow-through). The filtrate was lyophilized, dissolved in 95/3/0.1 v/v/v water/ acetonitril/formic acid and subsequently analyzed by on-line nanoHPLC MS/MS using an 1100 HPLC system (Agilent Technologies), as previously described ². Peptides were trapped at 10 µL/min on a 15-mm column (100-µm ID; ReproSil-Pur C18-AQ, 3 µm, Dr. Maisch GmbH) and eluted to a 200 mm column (50-µm ID; ReproSil-Pur C18-AQ, 3 µm) at 150 nL/min. All columns were packed in house. The column was developed with a 30-min gradient from 0 to 50% acetonitrile in 0.1% formic acid. The end of the nanoLC column was drawn to a tip (ID ~5 µm), from which the eluent was sprayed into a 7-tesla LTQ-FT Ultra mass spectrometer (Thermo Electron). The mass spectrometer was operated in data-dependent mode, automatically switching between MS and MS/MS acquisition. Full scan MS spectra were acquired in the FT-ICR with a resolution of 25,000 at a target value of 3,000,000. The two most intense ions were then isolated for accurate mass measurements by a selected ion monitoring scan in FT-ICR with a resolution of 50,000 at a target accumulation value of 50,000. Selected ions were fragmented in the linear ion trap using collision-induced dissociation at a target value of 10,000. In a post-analysis process, raw data were first converted to peak lists using Bioworks Browser software v 3.2 (Thermo Electron), then submitted to the Swissprot database using Mascot v. 2.2.04 (www.matrixscience.com) for protein identification. Mascot searches were with 2 ppm and 0.8 Da deviation for precursor and fragment mass, respectively, and no enzyme specified. Collision-induced dissociation spectra were manually inspected (see Supporting Information Figure S2.1B)

Human Ag presentation assays with apoptotic HeLa cells

Ag presentation to HIV- and vaccinia-specific human CD8 T-cells was studied using MoDC cross-presenting Ag from HeLa cells that were infected with NYVAC-C as described by

Quakkelaar et al. ³. The cytokine production of HIV-specific CD8 T-cells was assessed. In brief, HeLa cells were harvested by EDTA and infected with NYVAC-C or NYVAC-WT at a MOI of 5 for 1 hour. Cells were extensively washed to remove residual virus. After overnight incubation, cells were irradiated with UV-C (200 $\mu\text{W}/\text{cm}^2$) to ensure that no residual virus and no viable cells were present and thus exclude direct presentation. Apoptotic virus-infected HeLa cells were harvested and added to MoDC at a 2:1 ratio. After 6 hr incubation, HIV- or vaccinia-specific CD8 T-cells were added (at approximately 5 T-cell: 1 DC ratio) followed by overnight culture at 37°C/5%CO₂. Brefeldin A (10 $\mu\text{g}/\text{ml}$, Sigma-Aldrich) was added to retain cytokines within the T-cells allowing the detection of multiple cytokines. After 18 hr, intracellular cytokine staining (ICS) was performed as described ⁴. Cells were fixed and permeabilized using Cytofix/Cytoperm™ Fixation/Permeabilization Solution Kit (BD). Cells were then incubated with α -TNF PE-Cy7 (clone MAb11, eBiosciences), α -IFN- γ FITC, α -IL-2 APC, α -MIP-1 β PE (all three from BD) and α -CD8 PerCP (Dako). After washing, cells were analyzed by flow cytometry using a LSRII flow cytometer (BD Pharmingen) and analyzed with FlowJo software (Treestar). Cells were first gated based on the characteristics forward and side scatter properties, followed by identification of CD3⁺CD8⁺ T cells followed by intracellular analysis of cytokines produced within the gated CD8⁺ T cells. Net accumulation of activated GAG-specific CD8⁺ T-cells is the percentage of live CD8⁺ cells expressing one or more of the analyzed cytokines upon stimulation with MoDC loaded with apoptotic NYVAC-C-infected HeLa cells. Background levels of cytokine production were determined, and subtracted from percentages obtained by GAG-specific stimulation, by culturing GAG-specific CD8⁺ T-cells with MoDC incubated with NYVAC-WT infected HeLa.

Analysis of dendritic cell lysates incubated with fluorescent SLP by Tricine-SDS-PAGE

DC in 2 ml medium containing 2×10^6 cells were incubated with SLP-OVA_{31aa}-Bodipy for 24 hr. After incubation, cells were harvested and washed twice with PBS to remove non-internalized excess Ag. Supernatant was removed, the cell pellet resuspended in 50 μl lysis buffer (LB) (pH 7,4) and stored in eppendorf tubes at -80°C till further use. Cell lysates were subsequently obtained by repetitive freeze-thaw cycles by placing tubes for 30 sec in liquid nitrogen followed by 30 sec in heating blocks (eppendorf thermostat plus) set at 60°C. Cell lysates were analyzed using Tricine-SDS-PAGE gel as described before ⁵ with minor modifications. Briefly, 15 μl cell lysate was then mixed in a 1:1 ratio with *reducing* sample buffer and heated to 95°C for 10 minutes. Samples were next loaded onto a 1.5

mm SDS-PAGE gel (49.5%T 3%C stacking gel and 49.5%T 6%C separating gel). Samples were ran at 90 V through the stacking gel and followed by 5 hr run at 35 V through the separating gel (Biorad systems). Protein and peptides fragments where visualized using Coomassie (Supporting Information Figure S2.3A). Green-fluorescent fragments were imaged and analyzed for *EPI fluorescence intensity* applying *IVIS Imaging Systems*, measuring the fluorescence at 520nm emission wavelength (Supporting Information Figure S2.3B).

PLGA-SLP preparation

Poly-(lactic-co-glycolic-acid) (PLGA) nanoparticles loaded with SLP-OVA_{24aa} were prepared using a double emulsion with solvent evaporation method ⁶.

MHC class I Ag presentation by soluble SLP compared to SLP encapsulated in PLGA-NP in the presence of epoxomicin

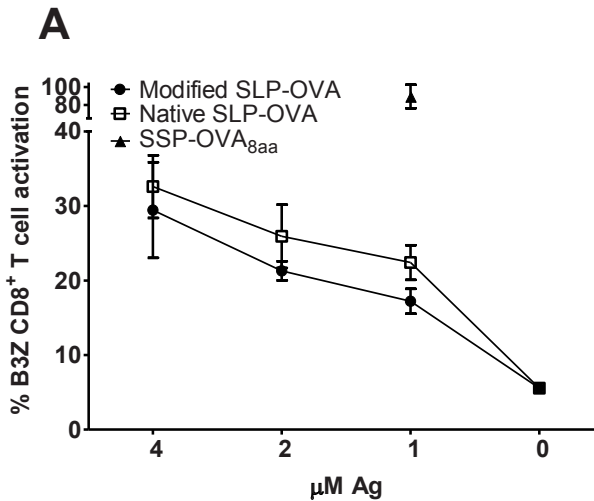
BMDC were left untreated or pre-incubated with 1 μ M *epoxomicin* (324800, Merck) incubated for 24 hr with SSP, SLP or protein or SLP encapsulated in PLGA-NP at the indicated concentrations. Cells were washed three times with medium before the T-cell hybridoma B3Z CD8⁺ T-cells were added followed by O/N incubation at 37°C. MHC class I Ag presentation of OVA₂₅₇₋₂₆₄ in H-2K^b was detected by activation of B3Z cells.

MHC class I Ag presentation by DC in the presence of Bafilomycin or in the absence of Cathepsin S

BMDC were left untreated (A) or pre-incubated with 50 nM of bafilomycin A1 (196000, Merck) followed by Ag-incubation as described above in the presence of the compound (B). Cells were washed three times with medium before the T-cell hybridoma B3Z CD8⁺ T-cells were added followed by O/N incubation at 37°C. BMDC from cathepsin S-deficient (Cathepsin KO) mice were cultured in the presence of titrated amounts of SLP-OVA_{24aa} and SSP-OVA_{8aa} followed by analysis of B3Z CD8⁺ T-cell activation after co-culture with Ag loaded BMDC (C). MHC class I Ag presentation of OVA₂₅₇₋₂₆₄ in H-2K^b was detected by activation of B3Z CD8⁺ T cells.

References

1. Crimmins DL, Mische SM, Denslow ND 2005. Chemical cleavage of proteins in solution. *Curr Protoc Protein Sci.* Chapter 11: Unit.
2. Meiring HD, van der Heeft E, ten Hove GJ, de Jong APJM 2002. Nanoscale LC-MS(n): technical design and applications to peptide and protein analysis. *J Sep Science* 25:557-568.
3. Quakkelaar ED, Redeker A, Haddad EK, Harari A, McCaughey SM, Duhon T, Filali-Mouhim A, et al. 2011. Improved innate and adaptive immunostimulation by genetically modified HIV-1 protein expressing NYVAC vectors. *PLoS One* 6:e16819.
4. Jing L, McCaughey SM, Davies DH, Chong TM, Felgner PL, De Rosa SC, et al. 2009. ORFeome approach to the clonal, HLA allele-specific CD4 T-cell response to a complex pathogen in humans. *J Immunol Methods* 347:36-45.
5. Schagger H 2006. Tricine-SDS-PAGE. *Nat Protoc* 1:16-22.
6. Silva AL, Rosalia RA, Sazak A, Carstens MG, Ossendorp F, Oostendorp J, Jiskoot W 2013. Optimization of encapsulation of a synthetic long peptide in PLGA nanoparticles: low burst release is crucial for efficient CD8+ T cell activation. *Eur J Pharm Biopharm* 83:338-345.



Supporting Information Figure S2.1A Similar processing and MHC class I presentation by DC of native and modified SLP-OVA_{24aa}*

WT BMDC were incubated for 24 hr with titrated amounts of native SLP-OVA with C-terminus sequence TEWTS or the SLP-OVA_{24aa} (see Table 2.1 in manuscript), washed 3x to remove excess Ag and co-cultured overnight in the presence of B3Z CD8⁺ T cells. T-cell activation was determined as described in M&M.

B

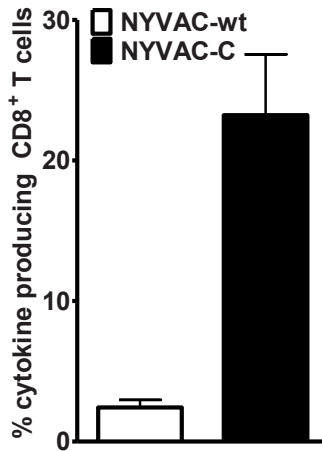
```

1  MGARASVLSG  GELDRWEKIR  LRPGGKKKYK  LKHIVWASRE  LERFAVNPGL
51  LETSEGCVRQI  LGQLQPSLQT  GSEELRSLYN  TVATLYCVHQ  RIEIKDTKEA
101 LDKIEEEQNK  SKKKAQQAAA  DTGHSNQVSQ  NYPIVQNIQG  QMVHQAI SPR
151 TLNAWVKVVE  EKAFSPEVIP  MFSALSEGAT  PQDLNTMLNT  VGGHQAAQM
201 LKETINEEAA  EWDRVHPVHA  GPIAPGQMR  PRGSDIAGTT  STLQE QIGWM
251 TNNPPIPVGE  IYKRWII LGL  NKIVRMYSP  T  SILDIRQGPK  EPFRDYVDRF
301 YKTLRAEQAS  QEVKNWMTET  LLVQANPDC  KTILKALGPA  ATLEEMMTAC
351 QGVGGPGHKA  RVLAEAMSQV  TNSATIMMQR  GNFRNQRKIV  KCFNCGKEGH
401 TARNCRAPRK  KGCWKCGKEG  HQMKDCTERQ  ANFLGKIWPS  YKGRPGNFLQ
451 SRPEPTAPPE  ESFRSGVETT  TPPQKQEPID  KELYPLTSLR  SLFGNDPSSQ
501
..... = GPGHKARVL-epitope sequence presented in HLA-B7 and
recognized by the HIV-specific CD8+ T cell clone

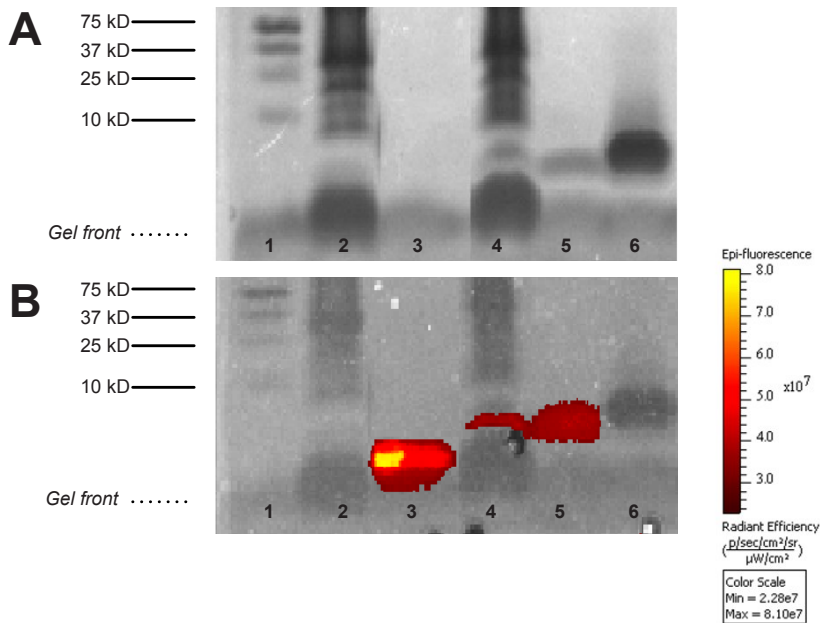
```

Supporting Information Figure S2.1B HIV-1 GAG-protein Identification by Mass Spectrometry.

HIV-GAG protein was digested with CNBr and endoproteinase GluC and analyzed by mass spectrometry (MS) as described in Supporting Information M&M. Full scan MS spectra were acquired. In a post-analysis process, raw data were first converted to peak lists using Bioworks Browser software v 3.2 (Thermo Electron), then submitted to the Swissprot database using Mascot v. 2.2.04 (www.matrixscience.com) for protein identification.

HLA-B7/GPGHKARVL CD8⁺ T cell activation**Supporting Information Figure S2.2 CD8⁺ T cell recognition of processed native GAG-protein presented by human DC loaded with apoptotic HeLa cells.**

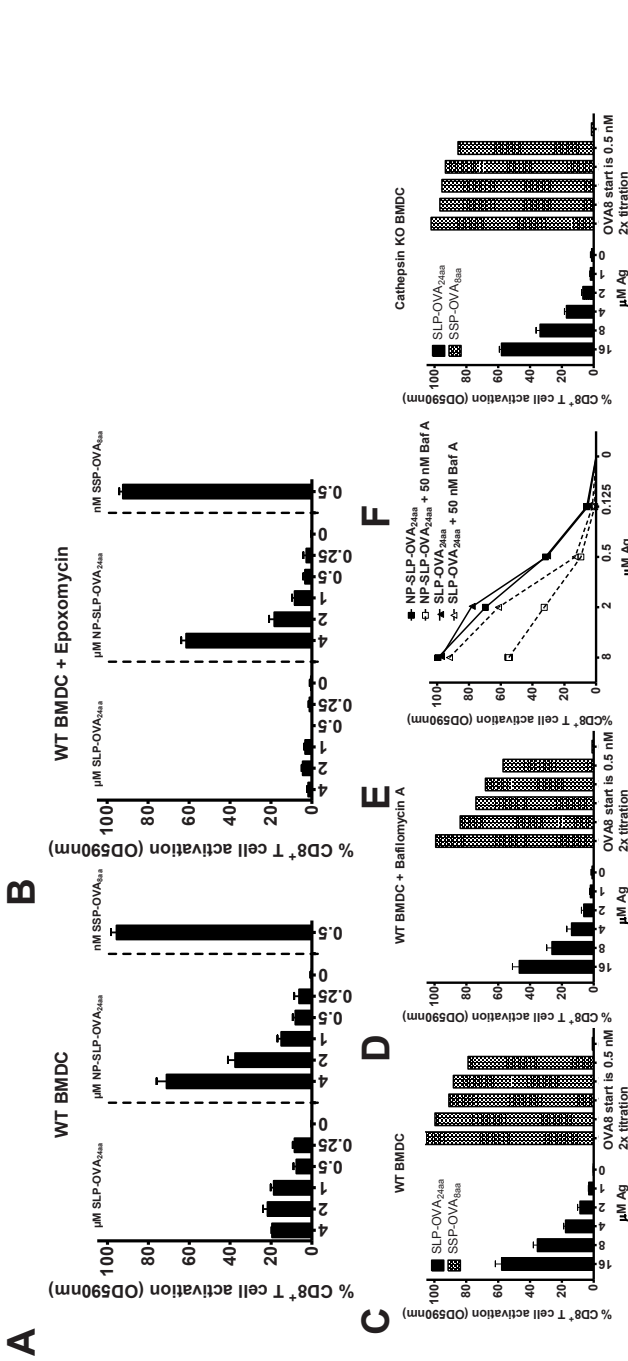
HeLa cells were harvested by EDTA and infected with NYVAC-C or NYVAC-WT at a MOI of 5 for 1 hour. Cells were extensively washed to remove residual virus. After overnight incubation, cells were irradiated with UV-C (200 $\mu\text{W}/\text{cm}^2$) to ensure that no residual virus and no viable cells were present and thereby excluding direct presentation. Apoptotic virus-infected HeLa cells were harvested and added to MoDC at a 2:1 ratio. After 6 hr incubation, HIV- or vaccinia-specific CD8 T-cells were added (at approximately 5 T-cell: 1 DC ratio) followed by overnight culture at 37°C/5%CO₂. Brefeldin A (10 $\mu\text{g}/\text{ml}$, Sigma-Aldrich) was added to retain cytokines within the T-cells allowing the detection of multiple cytokines. After 18 hr, intracellular cytokine staining was performed. Cells were fixed and permeabilized using Cytotfix/Cytoperm™ Fixation/Permeabilization Solution Kit (BD). Cells were then incubated with anti-TNF PE-Cy7 (clone MAb11, eBiosciences), anti-IFN- γ FITC, anti-IL-2 APC, anti-MIP-1 β PE (all three from BD) and anti-CD8 PerCP (Dako). After washing, cells were analyzed by flow cytometry using a LSRII flow cytometer (BD Pharmingen) and analyzed with FlowJo software (Treestar).



- 1) Resolution of the Bio Rad Precision plus Protein all blue standard protein kit 250 kD- 10 kD in 49,5%T, 3%C gel.
- 2) Cellysate of DC mock incubation
- 3) soluble SLP-OVA_{8aa}-Bodipy-FL
- 4) Cellysate of DC incubated with SLP-OVA_{31aa}-Bodipy-FL for 24 hr
- 5) soluble SLP-OVA_{31aa}-Bodipy-FL
- 6) soluble SLP-OVA_{31aa}

Supporting Information Figure S2.3 SLP-Bodipy-FL are intact upon internalization by DC.

DC in 2 ml medium containing 2×10^6 cells were incubated with SLP-OVA_{31aa}-Bodipy for 24 hr. After incubation, cells were harvested and washed twice with PBS to remove non-internalized excess Ag. Supernatant was removed, the cell pellet resuspended in 50 μ l lysis buffer (LB) (pH 7,4) and stored in eppendorf tubes at -80°C till further use. Cell lysates were subsequently obtained by repetitive freeze-thaw cycles by placing tubes for 30 sec in liquid nitrogen followed by 30 sec in heating blocks (eppendorf thermostat plus) set at 60°C . Cell lysates were analyzed using Tricine-SDS-PAGE gel as described before (35) with minor modifications. Briefly, 15 μ l cell lysate was then mixed in a 1:1 ratio with *reducing* sample buffer and heated to 95°C for 10 minutes. Samples were next loaded onto a 1.5 mm SDS-PAGE gel (49.5%T 3%C stacking gel and 49.5%T 6%C separating gel). Samples were ran at 90 V through the stacking gel and followed by 5 hr run at 35 V through the separating gel (Biorad systems). Protein and peptides fragments where visualized using Coomassie (Supporting Information Figure S2.2A). Green-fluorescent fragments were imaged and analyzed for *EPI fluorescence intensity* applying *IVIS Imaging Systems*, measuring the fluorescence at 520nm emission wavelength.



Supporting Information Figure S2.4 MHC class I presentation of soluble SLP is modulated by epoxomicin but not by Bafilomycin A and Cathepsin S.

BMDC were left untreated or pre-incubated with 1 μM *epoxomicin* (324800, Merck) incubated for 24 hr with SSP, SLP (A) or protein or SLP encapsulated in PLGA-NP (B) at the indicated concentrations. BMDC were left untreated (C) or pre-incubated with 50 nM of bafilomycin A1 (196000, Merck) followed by Ag-incubation as described above in the presence of the compound (D & E). Cells were washed three times with medium before the T-cell hybridoma B3Z CD8⁺ T-cells were added followed by O/N incubation at 37°C. BMDC from cathepsin S-deficient (Cathepsin KO) mice were cultured in the presence of titrated amounts of SLP-OVA_{24aa} and SSP-OVA_{24aa} followed by analysis of B3Z CD8⁺ T-cell activation after co-culture with Ag loaded BMDC (F). Cells were washed three times with medium before the T-cell hybridoma B3Z CD8⁺ T-cells were added followed by O/N incubation at 37°C. MHC class I Ag presentation of OVA₂₅₇₋₂₆₄ in H-2K^b was detected by activation of B3Z cells.

